Pis'ma v ZhETF, vol. 93, iss. 12, pp. 807 – 812 © 2011 June 25

Triplet p-wave superconductivity in low-density extended Hubbard model with Coulomb repulsion

M. Yu. Kagan[+], *D. V. Efremov*[*], *M. S. Marienko*[△], *V. V. Val'kov*[□]

[+] *P.L. Kapitza Institute for Physical Problems RAS, 119334 Moscow, Russia*

[*] *Max-Planck-Institut für Festkörperforschung, D-70569 Stuttgart, Germany*

[△] *Department of Physics and Astronomy, Hofstra University, Hempstead, 11549 New York, USA*

[□] *Kirenskii Institute of Physics, 660036 Krasnoyarsk, Russia*

Submitted 11 May 2011

We analyze superconducting instabilities in 3D and 2D extended Hubbard model with Coulomb repulsion between electrons on neighboring sites in the limit of low electron density ($n_{el} \to 0$) on simple cubic (square) lattice. We show that in a realistic strong-coupling case $U \gg V \gg W$ (U and V are the onsite and the intersite Coulomb repulsions, W the bandwidth) the main SC instability corresponds to the p-wave pairing and in the leading order is correctly described by the equations obtained earlier in the absence of the intersite Coulomb interaction $V = 0$.

1. Introduction. One of the main challenges of the modern condensed matter physics is to identify the origin of superconductivity in superfluid ^{3}He, heavy fermion compounds and Sr_2RuO_4, semimetals and superlatices. A lot of the experimental data as well as theoretical calculations suggest that the pairing results from the electron-electron interaction. In this scenario, a Coulomb repulsion is inverted into attraction due to the fermion background and retardation effects. This was first suggested by Kohn and Luttinger [1] for a 3D-system with point-like repulsion. The authors of Refs. [2–4] extended the analysis to 2D-systems and took into account the effects of long range Coulomb interaction in dense electron plasma. Recently, the question about the role of full Coulomb interaction for non-phonon mechanisms of superconductivity was raised in connection with the HTSC-physics by Alexandrov and Kabanov [5], and it still demands very thorough investigations both in the jellium and lattice models.

In the present paper we consider the simplest and the most repulsive (thus the most unfavorable for effective attraction and SC) lattice model with the strong on-site Hubbard repulsion U and the relatively strong additional Coulomb repulsion V on the neighboring sites (Fig. 1). We show that in this model the p-wave superconductivity exists in both the 3D- and 2D-case [2–4]. We assume the following estimates: $U \sim e^2/\varepsilon a_B$ for Hubbard U and $V \sim e^2/\varepsilon d$ for Coulomb V. Here $a_B \sim \varepsilon/me^2$ is the Bohr radius, ε the effective dielectric permittivity, d the intersite distance. We assume that for $\varepsilon \sim 1$: $a_B \sim 0.5$ Å, and $d \sim 3$–4 Å.

In the simple 3D cubic lattice the bandwidth is $W = 12t$ where t is the hopping integral, and the

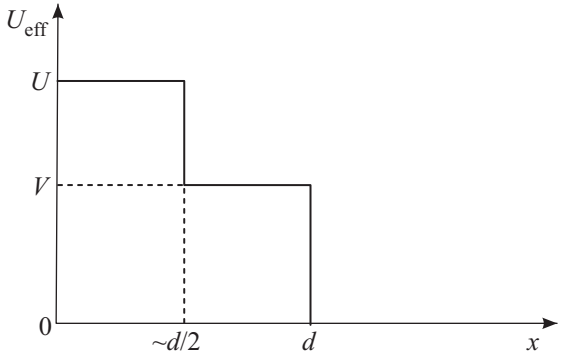

Fig. 1. Effective interaction in the extended Hubbard model with Coulomb interaction on neighboring sites

electron mass at low density (practically, empty lattice) $m = 1/2td^2$. The uncorrelated electron spectrum $\varepsilon(p) = -2t(\cos p_x d + \cos p_y d + \cos p_z d)$ approximately has quadratic form $\varepsilon(p) = -W/2 + p^2/2m$. Similarly, the chemical potential measured from the bottom of the band reads $\mu = -W/2 + \varepsilon_F$, where $\varepsilon_F = p_F^2/2m$ is the Fermi energy, p_F the Fermi momentum. If, as usual, we assume $a_B \ll d$ (which, rigorously speaking, is valid at moderate values of $\varepsilon \geq 1$), then comparing the estimates for $U \sim e^2/\varepsilon a_B$, $V \sim e^2/\varepsilon d$, and $W \sim 1/md^2$ in the limit $a_B/d \ll 1$ we come to the following hierarchy of parameters:

$$U \gg V \gg W. \tag{1}$$

Note that some important SC-systems possibly including HTSC could have large values of ε and thus be in difficult intermediate regime.

In this paper we construct the theory for the SC-instability in the parameter range (1) and at low electron

density $n_{\rm el} \to 0$ (or subsequent gas parameter $p_{\rm F}d \ll 1$), neglecting an important question of the microscopic phase separation of Mott–Hubbard type [6, 7] with FM-polarons inside the AFM-matrix, and that of Verwey type [8, 9] with metallic polarons inside the charge-ordered matrix. These instabilities towards nanoscale phase separation arise in the model under condition (1) close to $n_{\rm el} \to 1$ for the Mott–Hubbard and $n_{\rm el} \to 1/2$ for the Verwey type of phase separation.

In the following we show that the leading SC-instability at $n_{\rm el} \to 0$ corresponds to the triplet p-wave pairing and in the leading order of the gas parameter [10] $p_{\rm F}d$ is described by the expressions obtained in Refs. [2–4] for the low density Hubbard model in the absence of Coulomb interaction (at $V = 0$). We review the 2D-case and present analogous results for the p-wave pairing in the strong coupling case [11, 12] which is also in accordance with the low-density Hubbard model in the absence of V (at $V = 0$).

2. The model.

We consider the Hamiltonian

$$\hat{H}' = \hat{H} - \mu\hat{N} = -t\sum_{<ij>\sigma} c^{\dagger}_{i\sigma}c_{j\sigma} + U\sum_i n_{i\uparrow}n_{i\downarrow} + \\ + \frac{V}{2}\sum_{<ij>} n_i n_j - \mu\sum_{i\sigma} n_{i\sigma}, \qquad (2)$$

where $n_{i\sigma} = c^{\dagger}_{i\sigma}c_{i\sigma}$ is the electron density on site i with spin projection σ. After Fourier transformation, the Hamiltonian reads:

$$\hat{H}' = \sum_{\mathbf{p}\sigma}[\varepsilon(p) - \mu]c^{\dagger}_{\mathbf{p}\sigma}c_{\mathbf{p}\sigma} + U\sum_{\mathbf{pp'q}} c^{\dagger}_{\mathbf{p}\uparrow}c^{\dagger}_{\mathbf{p'}+\mathbf{q}\downarrow}c_{\mathbf{p}+\mathbf{q}\downarrow}c_{\mathbf{p'}\uparrow} + \\ + \sum_{\mathbf{pp'q}\sigma\sigma'} V(\mathbf{p},\mathbf{p'})c^{\dagger}_{\mathbf{p}\sigma}c^{\dagger}_{\mathbf{p'}+\mathbf{q}\sigma'}c_{\mathbf{p}+\mathbf{q}\sigma'}c_{\mathbf{p'}\sigma}, \qquad (3)$$

where

$$V(\mathbf{p},\mathbf{p'}) = \\ = V[\cos(p_x - p'_x)d + \cos(p_y - p'_y)d + \cos(p_z - p'_z)d]. \qquad (4)$$

In analogy with Ref. [13] it is useful to expand the effective interaction $U_{\rm eff} = U + 2V(\mathbf{p},\mathbf{p'})$ into the sum of the s-wave and p-wave partial harmonics.

At the low density $pd \ll 1$ the expansion up to quadratic terms gives effective interactions for s-wave and p-wave harmonics correspondingly:

$$U^s_{\rm eff} = U + 6V + o(p^2d^2), \text{ and } U^p_{\rm eff} = 2V\mathbf{pp'}d^2. \qquad (5)$$

In the strong-coupling case $U \gg V \gg W$ it is convenient to renormalize $U^s_{\rm eff}$ and $U^p_{\rm eff}$ in terms of vacuum Kanamori T-matrices T_s and T_p [14]. To do that we solve the Bethe-Salpeter equation in vacuum [15]. This yields [4] in the low-energy sector:

$$T_s = \frac{(U+6V)d^3}{1 + (U+6V)d^3\int\frac{d^3p}{(2\pi)^3}\frac{1}{2\varepsilon_p}} \sim \frac{(U+6V)d^3}{(1+\beta_s)}, \qquad (6)$$

where $\beta_s \sim (U+6V)/8\pi t > 0$ is the Born parameter for the s-wave channel, and we neglect the antibound state which corresponds to the pole of the T-matrix at high energies $E \sim U$ [6, 16].

We can introduce the s-wave scattering length

$$a_s = \frac{mT_s}{4\pi} = \frac{T_s}{8\pi td^2} \sim \frac{\beta_s d}{(1+\beta_s)}, \qquad (7)$$

and in the strong-coupling limit $\beta_s \gg 1$, evidently, $a_s \sim d$ (see Ref. [4]).

Correspondingly, the 3D-gas parameter of Galitskii [10]:

$$\lambda_s = \frac{2a_s p_{\rm F}}{\pi} \approx \frac{2p_{\rm F}d}{\pi}. \qquad (8)$$

Note that the same result for the s-wave scattering length is valid in the strong-coupling low-density limit of the Hubbard model without Coulomb interaction $V = 0$.

Similarly, for the T-matrix in the p-wave channel

$$T_p = 2A_p\mathbf{pp'}d^2 \qquad (9)$$

we get

$$A_p = \frac{Vd^3}{1 + Vd^3\int\frac{d^3p}{(2\pi)^3}\frac{p^2d^2}{3}\frac{1}{2\varepsilon_p}} = \frac{Vd^3}{(1+\beta_p)}, \qquad (10)$$

where

$$\beta_p = \eta\frac{V}{W} > 0 \qquad (11)$$

is the dimensionless Born parameter for the p-wave channel and $\eta \sim 1$ is a numerical coefficient.

Introducing the p-wave scattering length

$$a_p = \frac{A_p}{8\pi td^2} = \frac{Vd}{8\pi t(1+\beta_p)} \qquad (12)$$

We obtain in the strong coupling case $\beta_p \gg 1$

$$a_p \sim d. \qquad (13)$$

Thus

$$\frac{mT_p}{4\pi} = 2a_p\mathbf{pp'}d^2 \sim d^3\mathbf{pp'} \sim d^3pp'\cos\theta, \qquad (14)$$

where $\theta = \widehat{\mathbf{pp'}}$, and thus the dimensionless p-wave gas parameter reads:

$$\lambda_p \sim p_{\rm F}d^3p_{\rm F}^2 \sim (p_{\rm F}d)^3. \qquad (15)$$

Note that the estimate (15) is natural for the p-wave harmonics of the scattering amplitude for slow ($p_{\rm F}d < 1$) particles in vacuum [15].

3. Bethe-Salpeter integral equation for T_c. According to Landau–Thouless criterion for SC [17],

$$\Gamma_l = \frac{\tilde{\Gamma}_l}{1 + \tilde{\Gamma}_l \ln\left(\frac{2e^C \varepsilon_{\rm F}}{\pi T_c}\right)}, \qquad (16)$$

where $C \approx 0.58$ is the Euler constant, Γ the total vertex for the Cooper channel, $\tilde{\Gamma}$ the irreducible bare vertex, and l the orbital moment of the Cooper pair.

The critical temperature T_c is given by the pole of (16). If $\tilde{\Gamma} < 0$ for several values of l, then the actual symmetry of the superconducting state corresponds to the highest T_c. According to Kohn and Luttinger [1], in the absence of the Coulomb interaction (i.e. of λ_p (15)) $\tilde{\Gamma}_{l\neq 0}$ is given by the sum of four irreducible diagrams (see Fig. 2) which are of the second order of the s-wave

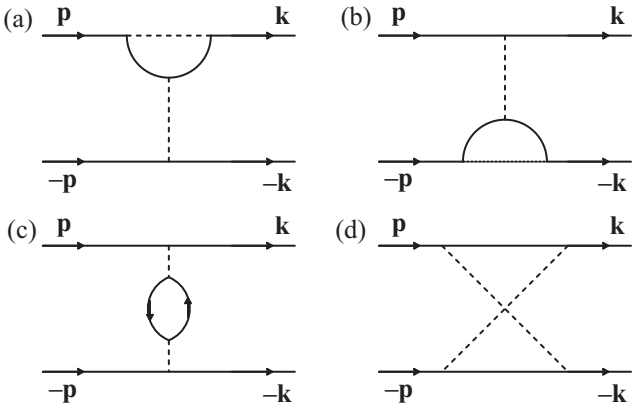

Fig. 2. Irreducible diagrams in the second order of the s-wave gas parameter λ_s which are nonzero only in the presence of fermion background (at $\varepsilon_{\rm F} \neq 0$)

gas parameter λ_s. At the same time, for $l = 1$ due to the presence of Coulomb repulsion V:

$$\tilde{\Gamma}_{l=1} = \lambda_s^2 \Pi^d_{l=1} + \lambda_p, \qquad (17)$$

where $\Pi^d = \Pi(\mathbf{p} + \mathbf{k})$ is the exchange diagram (see Fig. 2d.), λ_p is the bare vertex due to the p-wave vacuum contribution of the intersite Coulomb interaction V.

As shown in Ref. [1] for contact interaction λ_s the first three diagrams in the Fig. 2 exactly cancel each other, and the resulting $\tilde{\Gamma}_{l=1}$ is given by the fourth, exchange diagram (see (17)).

An exact evaluation of simple integrals shows [2–4] that for the exchange diagram $\lambda_s^2 \Pi^d_{l=1} = -\lambda_s^2/13 < 0$ which corresponds to the attraction and cannot be overcompensated by the repulsive bare vertex contribution $\lambda_p \sim \lambda_s^3$. This contribution only changes the next term in the expansion of $\tilde{\Gamma}_{l=1}$ in terms of gas parameter and, in fact, is the corrections to main exponent. To be specific (see Ref. [12, 18] and Fig. 3):

$$\tilde{\Gamma}_{l=1} = -\frac{\lambda_s^2}{13} - \left(\frac{\lambda_s^3}{3} - \lambda_p\right) + o(\lambda_s^4). \qquad (18)$$

Let us repeat again that the result (18) with the bare vertex $\lambda_p \sim \lambda_s^3 \sim (p_{\rm F}d)^3$ is to some extent evident be-

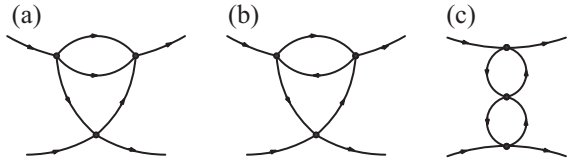

Fig. 3. Irreducible diagrams in the third order of gas parameter for the Cooper channel

cause according to quantum mechanics [15] for slow particles in vacuum the p-wave harmonic of the scattering amplitude is of the order $(ap_{\rm F})^{2l+1} \sim (ap_{\rm F})^3$ at $l = 1$ and $p \sim p_{\rm F}$. Thus the repulsive term in our case does not overcompensate the Kohn–Luttinger attractive contribution which arises only in fermion substance (when $\varepsilon_{\rm F} \neq 0$) and is proportional to $(ap_{\rm F})^2$. The only peculiarity of the lattice is that $a \sim d$ at the large Hubbard $U \gg W$ and at low density of electrons, and hence $\lambda_s^2 \sim (p_{\rm F}d)^2 \ll 1$.

Thus even at the most repulsive (and thus unfavorable for effective attraction and SC) hierarchy of parameters $U \gg V \gg W$ the presence of the Coulomb repulsion V does not change the main exponent for the p-wave critical temperature which reads $T_{c1} \sim \varepsilon_{\rm F} \exp\left(-13/\lambda_s^2\right)$ as in [2–4].

Note that if we change the hierarchy of parameters and make Coulomb repulsion weaker $W \gg U \gg V$, then in the Born case:

$$\lambda_p \sim \frac{mVd^2}{4\pi} p_{\rm F}^3 d^3 \sim \frac{mVd^2}{4\pi} \lambda_s^3 \sim \frac{V}{W} \lambda_s^3 \ll \lambda_s^2 \left(\frac{U + 6V}{W}\right)^2, \qquad (19)$$

for $p_{\rm F} \to 0$ and still the overcompensation of the Kohn–Luttinger attraction by the bare repulsion due to the intersite Coulomb interaction V is impossible. Thus, in the principal approximation in the gas parameter we restore the results on the possibility of the p-wave superconductivity obtained earlier in the absence of the intersite repulsion[2–4].

4. 2D extended Hubbard model. In the 2D extended Hubbard model with attractive interaction ($-V < 0$) on neighboring sites the vacuum T-matrices

for the s-wave and p-wave channels were obtained in the Refs. [13, 19]. After the substitution $-V \to V$ they yield for the s-wave channel $U^s_{\text{eff}} = U + 4V$ in the repulsive case $U \gg V \gg W$:

$$\frac{mT_s(\tilde{E})}{4\pi} \approx \frac{(U+4V)\left(md^2/4\pi\right)}{1+(U+4V)\left(md^2/4\pi\right)\ln\left(W\gamma/|\tilde{E}|\right)}, \tag{20}$$

where $\gamma \sim 1$ is the numerical coefficient. Again, we assume that we are in the low energy sector when one can neglect the second pole of the T_s which corresponds to the antibound state $E \approx U$ [6, 16]. In the Eq. (20) $W = 8t$ for the 2D square lattice, and the energy $\tilde{E} = E + W$ is measured from the bottom of the band. If $(U+4V)/W \ll 1$, then

$$\frac{mT_s(\tilde{E})}{4\pi} \approx \frac{1}{\ln\left(W\gamma/|\tilde{E}|\right)}. \tag{21}$$

In the Cooper problem $|\tilde{E}| = 2\varepsilon_F$ and with the logarithmic accuracy we restore the 2D dimensionless gas parameter of Bloom [20]:

$$f_s \approx \frac{1}{\ln\left(1/nd^2\right)}, \tag{22}$$

where $n = p_F^2/2\pi$ is the electron density in 2D.

Analogously, in the p-wave channel $U^p_{\text{eff}} = 2V\mathbf{pp}'d^2$, and the p-wave T-matrix reads:

$$\frac{mT_p}{4\pi} = \frac{2mA_p}{4\pi}\mathbf{pp}'d^2 = \frac{2mA_p}{4\pi}pp'd^2\cos\phi, \tag{23}$$

where $\phi = \widehat{\mathbf{pp}'}$, and

$$\frac{mA_p}{4\pi} = \frac{mVd^2}{(1+V/V_{cp})8\pi}. \tag{24}$$

Correspondingly [19],

$$V_{cp} = 11.2t \approx 1.4W. \tag{25}$$

At $V \gg V_{cp}$, the dimensionless p-wave scattering length in 2D reads

$$\frac{mA_p}{4\pi} = \frac{md^2V_{cp}}{8\pi}, \tag{26}$$

and, accordingly, the dimensionless p-wave gas parameter is

$$f_p \sim \frac{2mV_{cp}d^2}{8\pi}p_{\text{F}}^2d^2 \sim p_{\text{F}}^2d^2. \tag{27}$$

Thus $f_p \sim p_{\text{F}}^2d^2$ again in agreement with general quantum-mechanical results [15] for slow ($p_{\text{F}}d < 1$) particles in vacuum in the 2D-case.

5. The Cooper problem in 2D at low electron density and in the presence of intersite Coulomb repulsion. If we restrict ourselves to a very low electron density $n_{\text{el}}d^2 \ll 1$ and quadratic spectrum $\varepsilon(p) - \mu = (p^2 - p_F^2)/2m$, then in the second order of the s-wave gas parameter the irreducible vertex for the Cooper channel reads:

$$\tilde{\Gamma} = f_s^2\Pi(\mathbf{p}+\mathbf{k}). \tag{28}$$

However, the specific form of the polarization operator on quadratic spectrum in 2D [21] for $\mathbf{q} = \mathbf{p} + \mathbf{k}$

$$\Pi(q) = 1 - \text{Re}\sqrt{1 - 4p_{\text{F}}^2/q^2} \tag{29}$$

makes the large Kohn's anomaly ineffective for the SC-problem [4, 11]. Indeed, in the SC-problem $q \le 2p_{\text{F}}$, $\text{Re}\sqrt{1-4p_F^2/q^2} = 0$, and thus $\Pi(q) = 1$. Hence, the polarization operator does not depend on q, and correspondingly it does not contain harmonics with $l \neq 0$ (or more precisely, with the magnetic quantum number $m \neq 0$). Thus $\Pi_{m=1} = 0$, and SC arises only in the third order of f_s for quadratic spectrum (or in the second order of f_s if we take into account corrections $\left(p_x^4 + p_y^4\right)d^2/m$ which differ the exact spectrum on the square lattice $\varepsilon(p) = -2t(\cos p_x d + \cos p_y d) \approx \approx -W/2 + p^2/m - \left(p_x^4 + p_y^4\right)d^2/24m$ from the quadratic one $\varepsilon(p) = -W/2 + p^2/m$, see Ref. [22]). At very low density $n_{\text{el}} \to 0$ the third order terms in the quadratic spectrum from three irreducible diagrams in the Fig. 3 dominate over the quartic corrections to the spectrum.

Chubukov [11] found the leading contribution to $\tilde{\Gamma}_{m=1}$ from the first skeleton diagram in which the Cooper loop is inserted into the polarization loop (it is important that this diagram is still irreducible with respect to Cooper channel). Moreover, the character of the large 2D Kohn's anomaly in this diagram changes and it becomes $\text{Re}\sqrt{2p_{\text{F}} - q}$. Thus, the Kohn's anomaly becomes effective for SC in the third order. As a result he has obtained $\tilde{\Gamma}_{m=1} = -4.1f_s^3$ in the Ref. [11]. In the Ref. [12], all three irreducible skeleton diagrams on Fig. 3 were calculated numerically on equal ground. As a result, the exact vertex

$$\tilde{\Gamma}_{m=1} = -6.1f_s^3 \tag{30}$$

is even a little bit more attractive. The details of this calculation will be published in a separate article.

Thus, the total $\tilde{\Gamma}_{m=1}$ at $n_{el} \to 0$ reads:

$$\tilde{\Gamma}_{m=1} = -6.1f_s^3 + \alpha p_{\text{F}}^2d^2 + o(f_s^4), \tag{31}$$

where $\alpha \sim 1$ is a numerical coefficient.

Of course, keeping in mind that $f_s \sim 1/\ln\left(1/nd^2\right) \sim \sim 1/\ln\left(1/p_{\rm F}^2 d^2\right)$, we see that $f_s^3 \gg {p_{\rm F}}^2 d^2$ at $p_{\rm F} d \ll 1$. Thus, $\tilde{\Gamma}_{m=1} \approx -6.1 f_s^3$ just like in the case $V = 0$.

We can see again that in the strong-coupling limit $U \gg V \gg W$ of the extended Hubbard model on the square lattice and at low electron density $p_{\rm F} d \ll 1$ an inclusion of Coulomb repulsion does not change the main exponent for the p-wave critical temperature

$$T_{c1} \sim \varepsilon_{\rm F} \exp\left(-\frac{1}{6.1 f_s^3}\right). \qquad (32)$$

Thus in the principal order in the gas parameter we again restore the results on the p-wave superconductivity obtained earlier [11, 12] in the absence of the intersite Coulomb repulsion.

6. Discussions: the case of larger densities. If we increase the density in the 2D-case, we should remember that at $U \gg V \gg W$ the homogeneous metallic state stretches only up to the density $n_{\rm el} = 1/2 - \delta_c$, where in 2D $\delta_c \sim (W/V)^{1/2}$ (see Ref. [9]). At $n_{\rm el} > > 1/2 - \delta_c$ the system undergoes a phase transition into phase-separated state with metallic clusters inside charge-ordered checkerboard matrix (see Fig. 4).

Fig. 4. Phase separation at the density $n_{\rm el} \leq 1/2$ into metallic droplets in charge-ordered matrix

Note that at $n_{\rm el} = 1/2$ (quarter-filled band) we have Verwey localization (charge ordering) due to the condition $V \gg W$. Thus, we cannot extend our calculations for T_c in homogeneous case to densities larger than $n_{\rm el} = 1/2$. However, it is interesting to construct the SC phase diagram of the extended Hubbard model with the Coulomb repulsion on neighboring sites at the intermediate density $n_{\rm el} \leq 1/2$, and to find the regions that correspond to the p-wave, d_{xy}, and $d_{x^2-y^2}$ pairings [4, 22, 23].

Another interesting question would be to add to the model an infinite set of Coulomb repulsion terms with the amplitude decreasing with the distance between the sites: $V_2 n_i n_{i+2}$ on next-to-nearest sites with $V_2 < V$, $V_3 n_i n_{i+3}$ on next-to-next-to-nearest sites with $V_3 < V_2 < V$ etc. and to build a bridge between the extended Hubbard model and the jellium model for screened Coulomb interaction considered in Ref. [5].

We think, however, that at least at very low electron density $n_{\rm el} \to 0$ our results on the p-wave critical temperature will be stable in the main order of the gas parameter $p_{\rm F} d \ll 1$ in 3D and $1/\ln(1/p_{\rm F}^2 d^2)$ in 2D.

7. Conclusion. We considered the extended Hubbard model with Coulomb repulsion on the neighboring sites in the most repulsive (and thus the most unfavorable for effective attraction and SC) strong-coupling case $U \gg V \gg W$. In the limit of small electron density $p_{\rm F} d \ll 1$ we found that the p-wave contribution from the intersite Coulomb repulsion V to the irreducible bare vertex $\tilde{\Gamma}_{l=1}$ in the p-wave channel is proportional to $(p_{\rm F} d)^3$ in 3D and to $(p_{\rm F} d)^2$ in 2D in agreement with general quantum-mechanical results for slow particles in vacuum.

Thus both in 3D and 2D these repulsive terms cannot overcompensate attractive contributions which are proportional to $(p_{\rm F} d)^2$ in 3D and to $1/\ln^3(1/p_{\rm F}^2 d^2)$ in 2D. Note that the attractive contributions appear only in the presence of fermion background ($\varepsilon_{\rm F} \neq 0$). Thus the results of Refs. [4, 11, 12, 18] on the p-wave SC of Kohn–Luttinger type [5] both in 3D and 2D repulsive-U Hubbard model at low electron density and strong coupling $U \gg W$ are robust against the addition of even strong Coulomb repulsion on neighboring sites $V \gg W$ in the extended lattice models. Hence we can see that the p-wave superconductivity exists in purely repulsive models without electron-phonon interaction.

Note that we can strongly increase the p-wave critical temperature already at low density in a spin-polarized case [24] or in the two-band situation [25] and thus reach the realistic values of T_c (of the order of 1–5 K especially in the 2D or in layered systems [26]). The p-wave pairing is realized or can be expected in superfluid ^{3}He and ultracold Fermi-gasses, heavy fermion compounds and Sr_2RuO_4, semimetals and superlatices, layered dichalcogenides and organic superconductors [27–30].

We acknowledge useful discussions with A.V. Chubukov, A.S. Alexandrov, I.A. Fomin, K.I. Kugel and V.V. Kabanov. This work was supported by RFBR grants #11-02-00708 and #11-02-00741, M.S.M acknowledges the support by the Department of Energy under Award #DE-FG02-08ER64623 (Hofstra University Center for Condensed Matter).

1. W. Kohn and J.M. Luttinger, Phys. Rev. Lett **15**, 524 (1965).
2. D. Fay and A. Layzer, Phys. Rev. Lett. **20**, 187 (1968).
3. M. Yu. Kagan and A. V. Chubukov, JETP Lett. **47**, 525 (1988); A. V. Chubukov and M. Yu. Kagan, Jour. of Phys: Condens. Mat. **1**, 3135 (1989).
4. M. A. Baranov, A. V. Chubukov, and M. Yu. Kagan, Int. J. Mod. Phys. B **6**, 2471 (1992).
5. A. S. Alexandrov and V. V. Kabanov, Phys. Rev. Lett. **106**, 136403 (2011).
6. J. Hubbard, Proc. Roy. Soc. London A **276**, 238 (1963).

7. E. L. Nagaev, JETP Lett. **6**, 484 (1967); N. F. Mott and E. Davis, *Electronic Processes in Non-Crystalline Materials*, Clarendon Press, Oxford, 1971.
8. E. J. W. Verwey, Nature **144**, 327 (1939); E. J. W. Verwey and P. W. Haayman, Physica **8**, 979 (1941).
9. M. Yu. Kagan, K. I. Kugel, and D. I. Khomskii, JETP **93**, 415 (2001); M. Yu. Kagan and K. I. Kugel, Phys. Uspekhi **171**, 577 (2001).
10. V. M. Galitskii, JETP **34**, 151 (1958).
11. A. V. Chubukov, Phys. Rev. B **48**, 1097 (1993).
12. D. V. Efremov, M. S. Mar'enko, M. A. Baranov, and M. Yu. Kagan, Physica B **284-288**, 210 (2000); M. S. Mar'enko, PhD Thesis, Kapitza Institute, Moscow, 2000.
13. M. Yu. Kagan and T. M. Rice, J. Phys: Condens. Matter **6**, 3771 (1994); V. J. Emery, S. A. Kivelson, and H. Q. Lin, Phys. Rev. Lett. **64**, 475 (1990).
14. J. Kanamori, Progr. Theor. Phys **30**, 275 (1963).
15. L. D. Landau, E. M. Lifshitz, *Quantum Mechanics: Non-Relativistic Theory*, Pergamon, New York, 1977.
16. P. W. Anderson, Phys. Rev. Lett. **64**, 1839 (1990); Phys. Rev. Lett. **65**, 2306 (1990); Phys. Rev. Lett. **66**, 3226 (1991).
17. E. M. Lifshitz and L. P. Pitaevskii, *Statistical Physics*, Part 2, Pergamon, New York, 1980.
18. D. V. Efremov, M. S. Mar'enko, M. A. Baranov, and M. Yu. Kagan, JETP **90**, 861 (2000).
19. M. Yu. Kagan and D. V. Efremov, Phys. Rev. B **65**, 195103 (2002).
20. P. Bloom, Phys. Rev. B **12**, 125 (1975).
21. A. M. Afanas'ev and Yu. Kagan, JETP **43**, 1456 (1962).
22. M. A. Baranov and M. Yu. Kagan, Zeit. Phys. B – Condens. Matter **86**, 237 (1992).
23. M. Yu. Kagan, Habilitation Thesis, Kapitza Institute, Moscow (1994).
24. M. Yu. Kagan and A. V. Chubukov, JETP Lett. **50**, 517 (1989).
25. M. Yu. Kagan, Phys. Lett. A. **152**, 303 (1991).
26. M. Yu. Kagan and V. V. Val'kov, Sov. Low Temp. Phys **37**, 84 (2011); JETP **140**, 179 (2011).
27. D. Vollhardt and P. Woelfle, *The superfluid Phases of Helium 3*, Taylor and Francis, London (1990); G. E. Volovik, *Exotic Properties of Superfluid* ^{3}*He* , World Sci, Singapore (1992)
28. M. A. Baranov, M. Yu. Kagan, Yu. Kagan, JETP Lett. **64**, 301 (1996).
29. Y. Maeno, T. M. Rice, and M. Sigrist, Physics Today **54**, 42 (2001); T. M. Rice and M. Sigrist, J. Phys: Condens. Matter **7**, L643 (1995); H. R. Ott et al Phys. Rev. Lett. **52**, 1915 (1984); S. Kromer et al, Phys. Rev. Lett, **81**, 4476 (1998); H.-Y. Kee, A. Raghavan, and K. Maki, arxiv:condmat/0711.0929.
30. K. Murase, S. Ishida, S. Takaoka et al., Surface Science **170**, 486 (1986).